

Characterization of spatial heterogeneity in groundwater  
applications

PhD Thesis

Department of Geotechnical Engineering and Geo-Sciences (ETCG)

Technical University of Catalonia, UPC

Paolo Trincherò

February 2009



**HYDROGEOLOGY GROUP**  
TECHNICAL UNIVERSITY OF CATALONIA

## Chapter 4

# A new method for the interpretation of pumping tests in leaky aquifers\*

### 4.1 Introduction

#### 4.1.1 Motivation

Many complex geologic systems exist in which vertical fluxes through confining overlying and/or underlying layers are not negligible. These formations are commonly known as leaky or semiconfined aquifers. A classical example is that of alluvial multilayered aquifer-aquitard systems, which are present worldwide. The analysis of the drawdown caused by a pumping test in a leaky aquifer allows the estimation of representative hydraulic parameters of both the aquifer being tested and the aquitard through which it is recharged, which, in turn, are essential for the proper management of the aquifer, the accurate prediction of contaminant migration, assessing vulnerability, and risk assessment in general.

---

\*This chapter is based on the article: Trinchero, P., X. Sanchez-Vila, N. Coptý, and A. Findikakis (2008), A new method for the interpretation of pumping tests in leaky aquifers, *Ground Water*, 46(1), 133–143.

### 4.1.2 Leaky aquifer hydraulics

The first mathematical analysis of well hydraulics in leaky aquifers was developed by *Hantush and Jacob* [44]. The authors presented the analytical solution for the transient drawdown due to constant pumping rate in leaky aquifers based on a series of simplifying assumptions: vertical flow in the aquitard, horizontal flow in the aquifer, negligible storage in the aquitard, constant hydraulic head in the unpumped (recharging) aquifer, and a pumping well of infinitesimal radius that fully penetrates the pumped aquifer. Under such conditions, the drawdown becomes a function of the hydraulic parameters of the aquifer (transmissivity,  $T$  [ $L^2T^{-1}$ ], and storage,  $S$  [dimensionless]) and the conductance of the aquitard,  $C$  [ $T^{-1}$ ], defined as the ratio of the vertical hydraulic conductivity over the thickness of the aquitard,  $C = K'/b'$ . Alternatively the drawdown can be expressed as a function of the leakage factor,  $B$  [ $L$ ], which combines two of the previous hydraulic parameters, given by

$$B = \sqrt{\frac{Tb'}{K'}} \quad (4.1)$$

The solution of Hantush and Jacob formed the starting point in the development of pumping test interpretation techniques such as the Inflection Point Method [42] and the type curves method defined by *Walton* [99].

Some of the assumptions made by *Hantush* [42] were relaxed in subsequent studies. *Hantush* [45] accounted for the storage capacity of the aquitard. He obtained a series of type curves as a function of the leakage factor,  $B$ , and of a new parameter that depends on the storage of both the aquifer and the aquitard. *Neuman and Witherspoon* [68, 69] provided a more generic solution taking into account the aquitard storage as well as the drawdown in the unpumped aquifer. The assumption of zero well radius was relaxed by incorporating the large-diameter well theory and accounting for well bore skin [63]. All these solutions are based on the assumption that the

hydraulic parameters of individual layers are homogeneous.

## 4.2 Pump tests in heterogeneous media

In the last two decades several studies have focused on the interpretation of pumping tests in heterogeneous confined aquifers. A brief review of some of the more relevant findings are presented here. A comprehensive review was recently presented in [84].

Examples of earlier studies which take into account the heterogeneity of the medium were those of *Barker and Herbert* [3], *Butler* [11] and *Butler and Liu* [12]. Their main result was that in an aquifer with an inclusion embedded in a matrix of different hydraulic properties, for very large times the slope of the drawdown versus log time was not affected by the transmissivity of the inclusion. More recently, *Meier et al.* [62] analyzed numerically the meaning of the parameters obtained using the Cooper-Jacob method [15] to interpret pumping tests in heterogeneous confined aquifers. They found that for low to moderate levels of heterogeneity, the estimated transmissivity is very close to the geometric mean of the transmissivity field, while the estimated storage can vary by orders of magnitude depending on the location of the observation point. These results were confirmed analytically by *Sanchez-Vila et al.* [83].

Several researchers such as *Bourdet et al.* [10], *Horne* [48], *Bourdet* [9] proposed the interpretation of pumping tests using the time-derivative of the drawdown curve (diagnostic plot) which is more sensitive to changes caused by boundary conditions (impermeable or leaky limit, well-bore storage, skin effect).

By comparison relatively few papers have focused on the analysis of pumping tests in heterogeneous leaky aquifers. *Amin* [2] proposed a methodology for the estimation of the rate of leakage based on the analysis of the slope of the drawdown versus time curve. [18] developed an analytic relation that expresses the equivalent transmissivity (defined as the transmissivity of an equivalent homogeneous leaky aquifer system with the same pumping) for steady state flow towards a well

as a distance-dependent weighted average of the point transmissivity values in the vicinity of the well.

### 4.3 Brief review of existing methodologies

In this section we present a brief summary of two commonly used methodologies for the interpretation of pumping tests in homogeneous leaky aquifers, namely, the curve matching approach described in [99] and the inflection point method proposed by [42]. The aim is to set the basis for the proposed new interpretation method, and to stress how the different methods, classical and new, provide different parameter estimates when applied to heterogeneous media.

In order to illustrate the different methodologies we consider a simple synthetic example. The leaky aquifer system is identical to that defined by *Hantush and Jacob* [44]. We simulated a pumping test using the finite difference code MODFLOW 2000, version 1.11 [46]. The domain consists of uniform 481 by 481 grid cells each 1 m by 1 m. A fully penetrating well is located at the centre of the domain and pumps only from the semiconfined aquifer. A constant flow condition is imposed at the well, while constant head is prescribed at the external boundaries. The upper unconfined aquifer is assumed to be unaffected by the pumping.

In this work we are primarily concerned with the spatial variability of the transmissivity field, and how existing interpretation methods, derived for homogeneous aquifers, would perform when applied to heterogeneous ones. For this purpose a heterogeneous transmissivity field was generated. The natural logarithm transform of the transmissivity was modeled as a multivariate Gaussian random spatial function (RSF) with a stationary mean and exponential semi-variogram. The log-transmissivity field (Figure 4.1) was generated using the turning bands method [60]. The mean of the transmissivity field was assumed to be  $1m^2/day$ , the variance and the integral scale of the log-transmissivity are 1 and  $8m$  respectively. This corresponds to 8 grid cells per integral scale. Both the conductance of the aquitard and the storage coefficient of the aquifer are considered homoge-

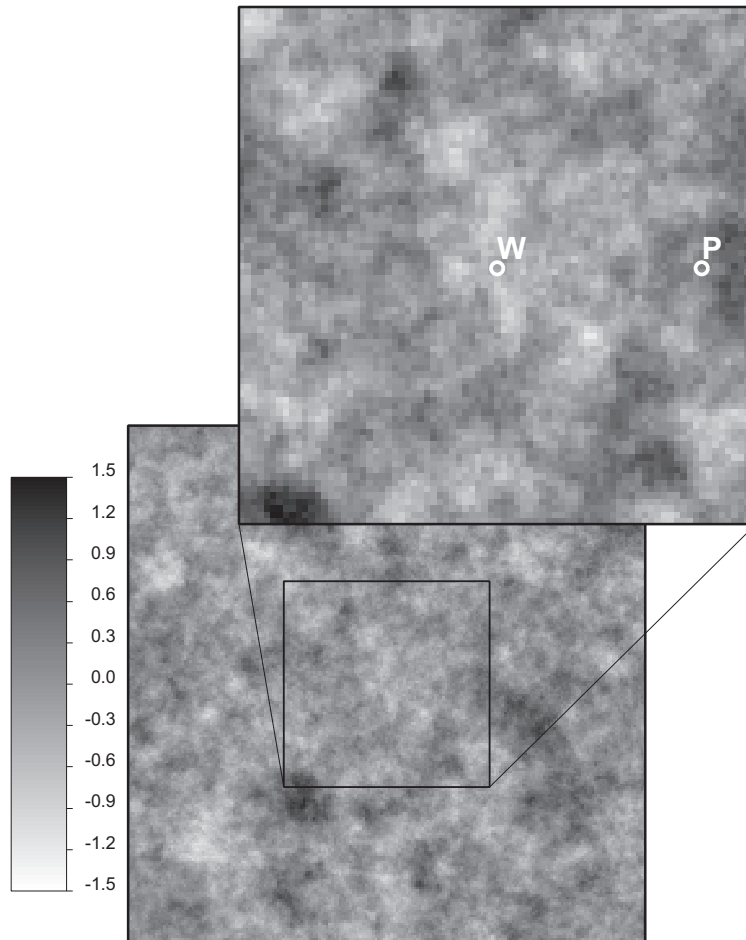


Figure 4.1: logarithm base-10 of the inner part of the transmissivity field (200 by 200 grid cells out of 481 X 481) and zoom around the well location. The well, W, and observation point, P, are indicated.

neous with values of  $10\text{day}$  and  $10$  respectively. We analyze the drawdown in a piezometer located at a distance of  $r = 32\text{m} (= 4I)$  from the well where is the integral scale of the semivariogram. The pumping rate,  $Q$ , is  $2\text{m}^3/\text{day}$ . Analysis of the simulated data indicated that the external boundaries were sufficiently far from the well such that they have no impact on the simulated transient drawdown at the observation point. Applying the curve fitting method [99] to the above example, we obtain the best match with  $r/B = 1.5$  (Figure 4.2 a) this means that the estimated parameters are

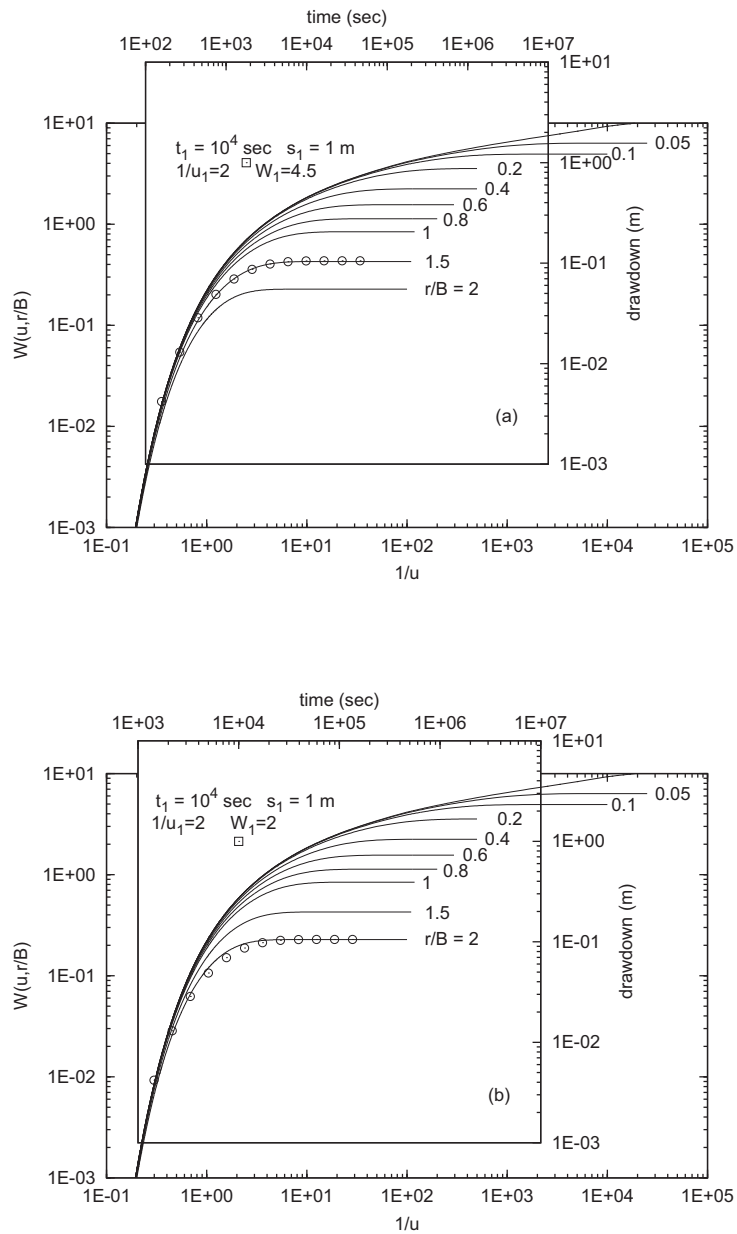


Figure 4.2: Interpretation of the synthetic pumping test using the type curve method of Walton [99]. The fit curve is that for (a)  $r/B = 1.5$  and (b)  $r/B = 2.0$  which shows the subjectivity of the curve matching method.

$$B_{est} = \frac{r}{1.5} \cong 21m$$

$$T_{est} = \frac{QW_1}{4\pi s_1} = \frac{2 \cdot 4.5}{4 \cdot \pi \cdot 1} \cong 0.7m^2/day$$

$$S_{est} = \frac{4T_{est}t_1u_1}{r^2} = \frac{4 \cdot 0.7 \cdot 0.11 \cdot 0.5}{32^2} \cong 1.6 \cdot 10^{-4}$$

$$C_{est} = \frac{T_{est}}{B_{est}^2} \cong 1.6 \cdot 10^{-3}day^{-1}$$

It is important to underline the uncertainty associated with the parameters estimated with this method. First, the process of curve superposition is rather subjective, particularly with imperfect field data, since the curves corresponding to different  $r/B$  values are quite similar in log-log scale. Second, the drawdown values corresponding to small times are usually noisy. Third, the apparent transmissivity influencing the drawdown changes as the pumping test progresses in time. As such, matching different parts of the pumping tests to the theoretical curves will lead to different estimates of the flow parameters.

Figure 4.2 (b) shows the match of the simulated drawdown data with the  $r/B = 2$  curve, which is almost as good as that with the  $r/B = 1.5$  curve. If the  $r/B = 2$  curve is selected as the best match, the following parameter values are obtained

$$B_{est} = \frac{r}{2} \cong 16m$$

$$T_{est} \cong 0.3m^2/day$$

$$S_{est} \cong 0.6 \cdot 10^{-4}$$

$$C_{est} \cong 1.2 \cdot 10^{-3}day^{-1}$$

The difference in the estimates of the leakage factor is more than 20%, which propagates



into the estimation of the transmissivity, storage coefficient and aquitard conductance resulting in differences of 50% – 60% with respect to their actual values, i.e. those used in the pumping test simulation.

The second method considered here is the inflection point method [42]. For the leaky aquifer system defined by *Hantush and Jacob* [44], this method expresses the ratio between the steady state drawdown,  $s_{steady}$ , and the slope of the tangent to the drawdown with respect to logarithm of time curve at the inflection point,  $m$ , as a function of the leakage factor

$$s_{steady}/m = 0.87 \frac{K_0(r/B)}{\exp(-r/B)} \quad (4.2)$$

where  $K_0$  is the modified Bessel function of the second kind of order zero. The position of the inflection point of the curve in a homogeneous medium is given by the following equation

$$t_{inf} = \frac{rBS}{2T} \quad (4.3)$$

and it is possible to demonstrate analytically that coincides with the time where half the steady state drawdown occurs. In heterogeneous conditions this coincidence does not generally hold.

For leaky aquifers, a proper steady-state drawdown regime is reached asymptotically with time. For a homogeneous leaky aquifer, the steady state drawdown is given by [22]

$$s_{steady} = \frac{Q}{2\pi T} K_0(r/B) \quad (4.4)$$

The monotonic curve obtained from equation (4.2) is plotted in Figure 4.3 which in real applications can directly provide an estimate of the leakage factor  $B$ , once the ratio  $s_{steady}/m$  is estimated from the observed drawdown data.

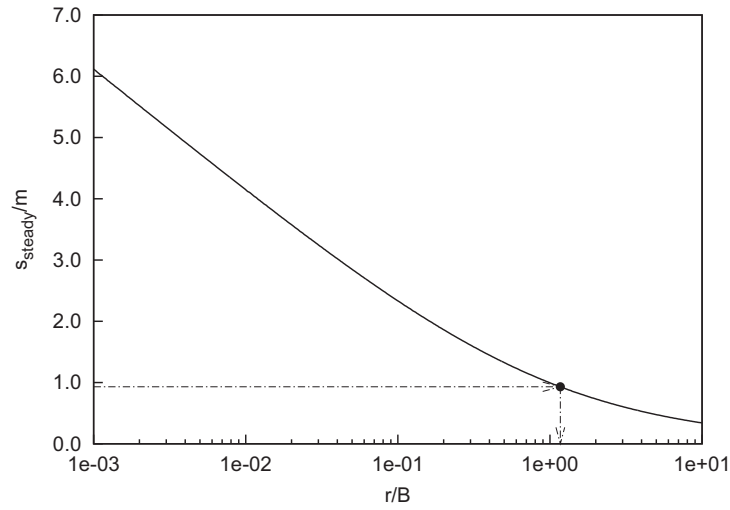


Figure 4.3: Plot of the ratio  $s_{steady}/m$  as a function of  $r/B$  (equation 4.2) used in the interpretation data with the inflection point method [42].

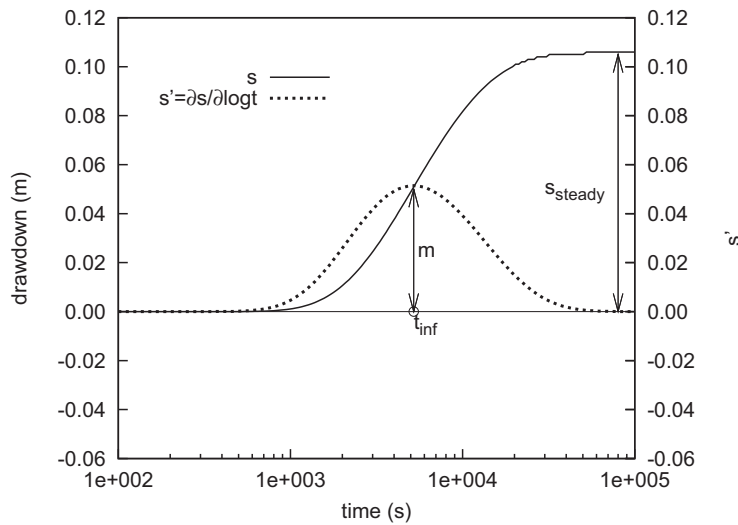


Figure 4.4: Drawdown in the synthetic pumping test and its first derivative.

Figure 4.4 shows the simulated drawdown of our example and the first derivative of the drawdown ( $m$ ) which was computed numerically from the simulated drawdown using central differences. From this Figure the ratio  $s_{steady}/m_i \cong 0.93$ , leading to  $B_{est} \cong 27m$ . The transmissivity was

estimated using equation (4.4) which yields a value of about  $1m^2/day$ . The storage coefficient is estimated using equation (4.3) as  $S_{est} \cong 8 \cdot 10^{-3}$ . The aquitard conductance is obtained indirectly from the estimates of  $T$  and  $B$ , leading to  $C_{est} \cong 1.2 \cdot 10^{-3} \text{ day}^{-1}$ .

It is important to emphasize that in a homogenous system the two methods would provide the same estimated parameters. In a heterogeneous system the estimated parameters would be different, since in the two methods of interpretation we focus on different parts of the drawdown vs time curve. Even if, strictly speaking, the superposition method uses the entire drawdown curve, the fitting process is strongly conditioned by the shape of the first part of the curve which is frequently biased by noise. On the other hand, the inflection point method uses both the transient and the steady state part of the test, but tends to disregard the early part of the curve (initial time behaviour) because only data of the second part of the transient drawdown curve are used in the estimation.

## 4.4 The Double Inflection Point Method

### 4.4.1 Assumptions and Methodology

The system considered in the development of this methodology is the same as that defined by *Hantush and Jacob* [44] and described above in the introduction. The two-dimensional flow equation that describes the problem, in radial coordinates, is as follows:

$$\frac{1}{r} \frac{\partial}{\partial r} \left( r \frac{\partial s}{\partial r} \right) - \frac{Cs}{T} = \frac{S}{T} \frac{\partial s}{\partial t} \quad (4.5)$$

where  $s(t, x, y)$  is the transient drawdown. The analytical solution was provided by [42]

$$s = \frac{Q}{4\pi T} W(u, r/B) \quad (4.6)$$

where  $u = r^2S/4Tt$  and  $W(u, r/B)$  is the Hantush well function

$$W(u, r/B) = \int_u^\infty \frac{1}{y} \exp\left(-y - \frac{r^2}{4B^2y}\right) dy \quad (4.7)$$

From equations (4.6), (4.7) and using the Leibniz Integral Rule, the derivative of the drawdown with respect to the base-10 logarithm of time can be written as

$$s' = \frac{\partial s}{\partial \log t} = 2.30t \frac{\partial s}{\partial t} = \frac{2.30Q}{4\pi T} \exp\left(-\frac{r^2S}{4Tt} - \frac{Tt}{B^2S}\right) \quad (4.8)$$

The second and third derivatives of the drawdown are respectively

$$s'' = \frac{\partial^2 s}{\partial \log t^2} = \left[ \frac{2.30^2 Q}{4\pi T} \exp\left(-\frac{r^2S}{4Tt} - \frac{Tt}{B^2S}\right) \right] \left( \frac{r^2S}{4Tt} - \frac{Tt}{B^2S} \right) \quad (4.9)$$

$$s''' = \frac{\partial^3 s}{\partial \log t^3} = \frac{2.30^3 Q t}{4\pi T} \exp\left(-\frac{r^2S}{4Tt} - \frac{Tt}{B^2S}\right) \cdot \left[ -\frac{r^2S}{4Tt^2} - \frac{T}{B^2S} + t \left( \frac{r^2S}{4Tt^2} - \frac{T}{B^2S} \right)^2 \right] \quad (4.10)$$

The position where the first derivative  $s'$  is maximum, which is also the inflection point of the  $s$  versus  $\log t$  curve, is uniquely given by equation 4.3.

The inflection points of the first derivative are determined by setting the third derivative equal to zero. The roots of this equation are given by those of the following fourth order polynomial

$$\left(\frac{T}{B^2S}\right)^2 t^4 - \left(\frac{T}{B^2S}\right) t^3 - \frac{1}{2} \left(\frac{r}{B}\right)^2 t^2 - \frac{r^2S}{4T} t + \left(\frac{r^2S}{4T}\right)^2 = 0 \quad (4.11)$$

Multiplying all terms by  $T^2/S$  and introducing equation 4.3, we can write an equation involving  $t_{inf}$ , the leakage factor and the distance from the well,

$$\begin{aligned} r^4 \left( \frac{t}{2t_{inf}} \right)^4 - r^3 B \left( \frac{t}{2t_{inf}} \right)^3 - \frac{r^4}{2} \left( \frac{t}{2t_{inf}} \right)^2 \\ - \frac{r^3 B}{4} \left( \frac{t}{2t_{inf}} \right) + \frac{r^4}{16} = 0 \end{aligned} \quad (4.12)$$

It is possible to show mathematically that equation 4.12 has two real and two complex roots. The real roots,  $t_{si1}$  and  $t_{si2}$ , are the two inflection points of the first derivative of the drawdown with respect to the logarithm of time (i.e. the maximum and minimum of the second derivative curve).

Equation 4.12 is linear with respect to the leakage factor,  $B$ . Consequently, by rearranging terms, we can express  $B$ , as a function of  $\tau_j = t_{sj}/2t_{inf}$  ( $j = 1, 2$ ):

$$B = \frac{\left( \tau_{Dj}^2 - \frac{1}{4} \right)^2 r}{\tau_{Dj} \left( \tau_{Dj}^2 + \frac{1}{4} \right)} \quad (4.13)$$

Hence, with the double inflection point (DIP) method, the leakage factor can be directly estimated from the time where the first derivative of drawdown with respect to log time is maximum,  $t_{inf}$ , and one of its two inflection points,  $t_{s1}$  or  $t_{s2}$ . This estimate of  $B$  combined with equation provides an estimate of  $T$ ;  $S$  is then estimated from equation 4.3.

It can be demonstrated (see Appendix 4.10) that

$$\tau_1 \cdot \tau_2 = 1/4 \quad (4.14)$$

#### 4.5. APPLICATION OF THE DIP METHOD TO THE SYNTHETIC PUMPING TEST 71

$$t_{s1} \cdot t_{s2} = t_{inf}^2 \quad (4.15)$$

which means that in a semilogarithmic plot, the position of the two inflection points,  $t_{s1}$  and  $t_{s2}$ , is symmetric with respect to the position of  $t_{inf}$  (Appendix 4.10).

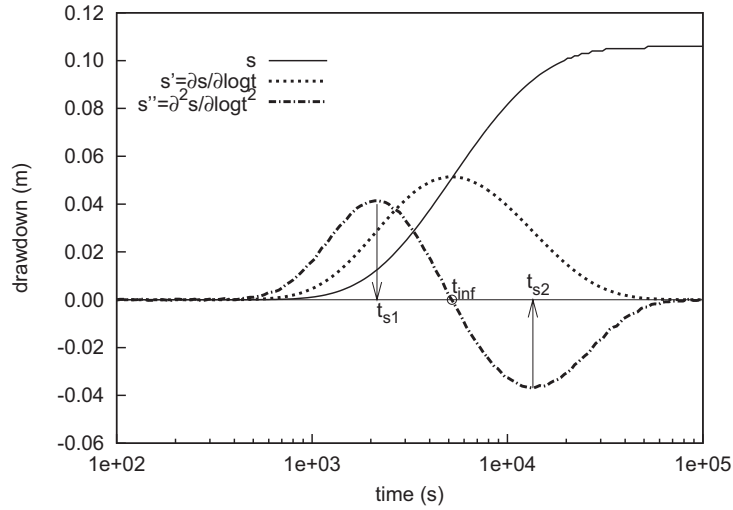


Figure 4.5: Interpretation of the synthetic example using the DIP method.

#### 4.5 Application of the DIP method to the synthetic pumping test

The DIP method is now applied to the synthetic pumping test data generated as described in the previous section. The drawdown versus time curve and its derivatives are presented on a semilog plot in Figure 5. From the derivatives, the position of the singular points was estimated as:

$$t_{s1} \cong 2150s \quad t_{s2} \cong 13500s \quad t_{inf} \cong 5200s \quad (4.16)$$

Two different values of the leakage factor were estimated depending on whether  $t_{s1}$  or  $t_{s2}$  are used in equation 4.13

$$B_{t_{s1}} \cong 23m \qquad B_{t_{s2}} \cong 26m \qquad (4.17)$$

The estimates of the other flow parameters are summarized in Table 6.1

	B(m)	T/S(m <sup>2</sup> /day)	T(m <sup>2</sup> /day)	S(-)	C(day <sup>-1</sup> )
Superposition	21	4450	0.7	$1.6 \cdot 10^{-4}$	$1.6 \cdot 10^{-3}$
Hantush inflection point	27	6650	1	$1.4 \cdot 10^{-4}$	$1.4 \cdot 10^{-3}$
DIP 1	23	6040	0.7	$1.2 \cdot 10^{-4}$	$1.3 \cdot 10^{-3}$
DIP 2	26	6970	0.9	$1.3 \cdot 10^{-4}$	$1.3 \cdot 10^{-3}$
DIP mean	24	6490	0.8	$1.2 \cdot 10^{-4}$	$1.3 \cdot 10^{-3}$
DIP graph.	25	6650	0.8	$1.2 \cdot 10^{-4}$	$1.2 \cdot 10^{-3}$
Geometric mean	31.6	10000	1	$1 \cdot 10^{-4}$	$1 \cdot 10^{-3}$
Value at well	25	6300	0.63	$1 \cdot 10^{-4}$	$1 \cdot 10^{-3}$

Table 4.1: summary of the results obtained with each method. DIP1 and DIP2 are the results obtained using the DIP method with  $t_{s1}$  and  $t_{s2}$  respectively. DIP mean refers to the geometric mean of DIP1 and DIP2. The geometric mean is the spatial mean of the parameter used in the generation of time-drawdown data.

## 4.6 DIP Method: A Graphical Approach

To develop a graphical procedure based on the DIP method, we define the following dimensionless variables

$$r_D = \frac{r}{B} \quad t_D = \frac{4Tt}{B^2S} \quad (4.18)$$

Combining Equations 4.14, 4.3 and 4.15 with the definition of  $\tau$  and the dimensionless definitions in Equation 4.18, the three singular points (maximum and the two inflection points) of the drawdown derivative curve can be written as follows

$$t_{D0} = \frac{4Tt_{inf}}{B^2S} = \frac{2r}{B} \quad (4.19)$$

$$t_{D1} = 2\tau_{D1}t_{D0} \quad (4.20)$$

$$t_{D2} = \frac{t_{D0}^2}{t_{D1}} \quad (4.21)$$

Since from equation 4.13 the variable  $\tau_{D1}$  is a function of  $r/B$  only, hence,  $t_{D0}$ ,  $t_{D1}$  and  $t_{D2}$  are all functions of  $r_D (= r/B)$  only. These relationships are shown in Figure 4.6 which can be used in a simple graphical procedure for the estimation of the leakage factor:

1. Given the time-drawdown data from a pumping test, estimate  $t_{inf}$ ,  $t_{s1}$  and  $t_{s2}$  (dimensional values).
2. Plot these three points on a vertical line with the same logarithm scale as the vertical axis of the type curves.
3. Slide the all three points together as a group across the diagram, i.e. keeping their positions relative to each other until each point falls on or close to its corresponding curve (Figure 4.6)
4. Read the value of  $r/B$  off the x-axis



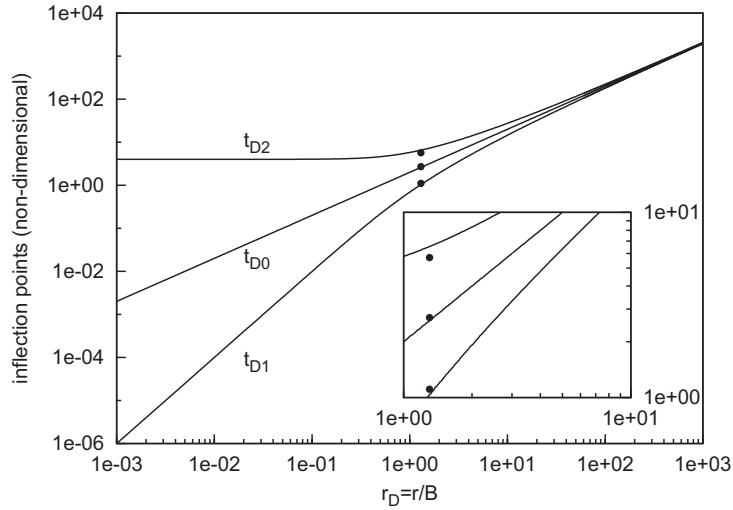


Figure 4.6: DIP graphical approach: type curves of  $t_{D0}$ ,  $t_{D1}$  and  $t_{D2}$  as a function of  $r/B$ . The points are the  $t_{inf}$ ,  $t_{s1}$  and  $t_{s2}$  values of the synthetic example. Note that because of the heterogeneity in the transmissivity field, it is not possible for the three points to simultaneously match the theoretical curves.

As noted in Equation 4.15,  $t_{s1}$  and  $t_{s2}$  are symmetric with respect to  $t_{inf}$  for homogeneous leaky aquifer systems. The departure of symmetry in the application of the graphical method is indicative of a heterogeneous leaky aquifer system.

For observation points not too far from the well (small  $r/B$  values), the three curves are sufficiently distinct for the flow parameters to be estimated and some information about the spatial variability of the transmissivity field may be inferred from the asymmetry of the point locations with respect to the type curves. At larger distances from the pumping well, all three curves converge towards  $t_{Di} = 2r/B$  ( $i = 0, 1, 2$ ) and the estimate of the leakage factor becomes indeterminate. This is also consistent with the sensitivity analysis of the DIP method presented in Figure 4.7 and Appendix 4.11 which shows that the error in the estimation of the leakage factor, increases rapidly for  $r/B$  values greater than 0.5.

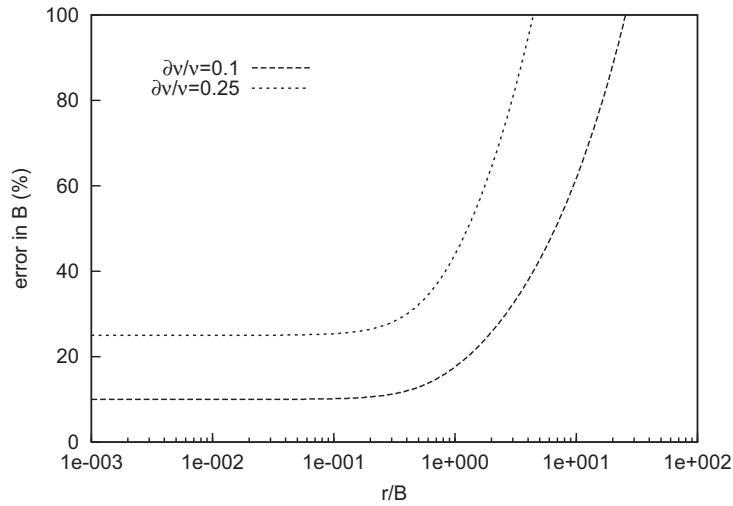


Figure 4.7: Percent error in the estimation of the leakage factor as a function of  $r/B$  for two different relative errors in the estimation of  $\tau_j$ .

#### 4.7 Comparison of the parameter values estimated with the different methods

Table 6.1 summarizes the estimated parameter values obtained with the various interpretation methods. These results show that in heterogeneous media different methods produce different estimates, none of which would necessarily matches the representative parameters of the system (defined by the constant input values for  $S$ ,  $C$  and some average value of  $T$ , for example the geometric mean,  $T_G$ ).

Further analysis of the actual transmissivity field can explain the variability in the estimated parameters. Figure 4.1 shows that the well is located in a zone of low permeability. Knowing that the characteristic time of a pumping test is inversely proportional to the transmissivity, we expect the drawdown curve (and consequently its derivatives) to be delayed with respect to the theoretical curve for an equivalent homogeneous medium. This is confirmed from Figure 8 where it can be observed that the delay diminishes with time, with the delay of larger that the delay of and the

delay of smaller than the delay of . This means that in this particular example is larger and is smaller than in the homogeneous case.

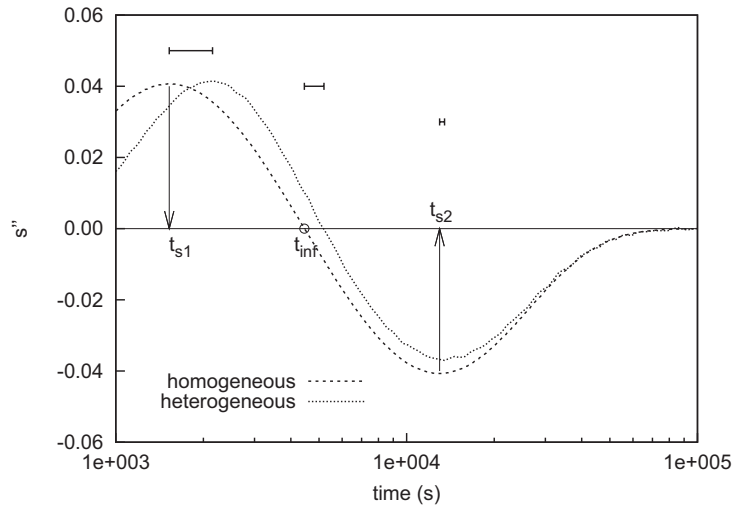


Figure 4.8: Second derivative of the drawdown from the synthetic pumping test in the heterogeneous aquifer and in the equivalent homogeneous aquifer (defined in terms of the geometric mean of the transmissivity field). The error bars show the shift of the singular points  $t_{inf}$ ,  $t_{s1}$  and  $t_{s2}$ .

The relationship between and the coefficient is shown in Figure 4.9. It consists of two monotonic curves: increases with  $\tau_1$  (always less than 0.5) while decreases with  $\tau_2$  (greater than 0.5). Since the spatial variability of the transmissivity in the example considered here leads to the overestimation of  $\tau_1$  and the underestimation of  $\tau_2$  relative to the homogeneous case, the leakage factor estimated with both  $t_{s1}$  and  $t_{s2}$  is smaller than that defined by the geometric mean of the transmissivity as confirmed from Table 6.1.

Similar effects can be seen in the other methods. Specifically we focus on the estimation of the leakage factor which is subsequently used in the estimation of the other flow parameters. The curve superposition method and the DIP1 method (DIP method using the first inflection point,  $t_{s1}$ ) are based mostly on the early portion of the time-drawdown data, which means that estimates of these methods are more indicative of the conditions near the well. Contrarily, the DIP2 method (DIP method using the second inflection point,  $t_{s2}$ ) uses the late and intermediate portions of the

drawdown curve, while the inflection point method deals with both the intermediate and steady (very late) portions of the data. Therefore, these two latter methods give information about a larger portion of the aquifer. Finally the DIP graphical method is a weighted estimate of both  $t_{s1}$  and  $t_{s2}$ .

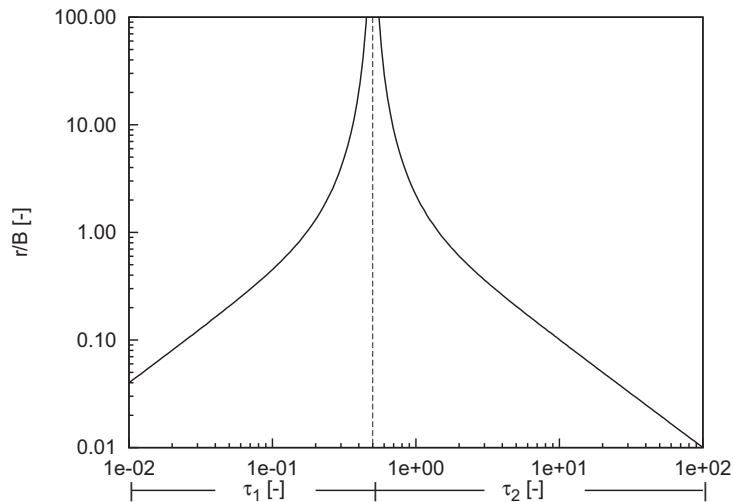


Figure 4.9:  $r/B$  as a function of the  $\tau_j$  values.

These qualitative considerations are confirmed quantitatively for the specific pumping test considered in the previous sections. Figure 4.10(a) shows how the estimated leakage factor depends on the portion of aquifer that is sampled. The leakage factor, which is defined based on the geometric mean of the transmissivity field, is larger than all the estimates, with the DIP2 and the Hantush inflection point estimates closest to the spatial mean. Similar trends are observed when analyzing the estimates of transmissivity from the different methods (Table 6.1 and Figure 4.10b). The DIP1 and the superposition methods lead to a value which is lower than  $T_G$ . The estimates obtained with the inflection point method and DIP2 yields values that are still lower, but closer to  $T_G$ , indicating that these transmissivity estimates are representative of the transmissivity of the entire aquifer than that close to the well

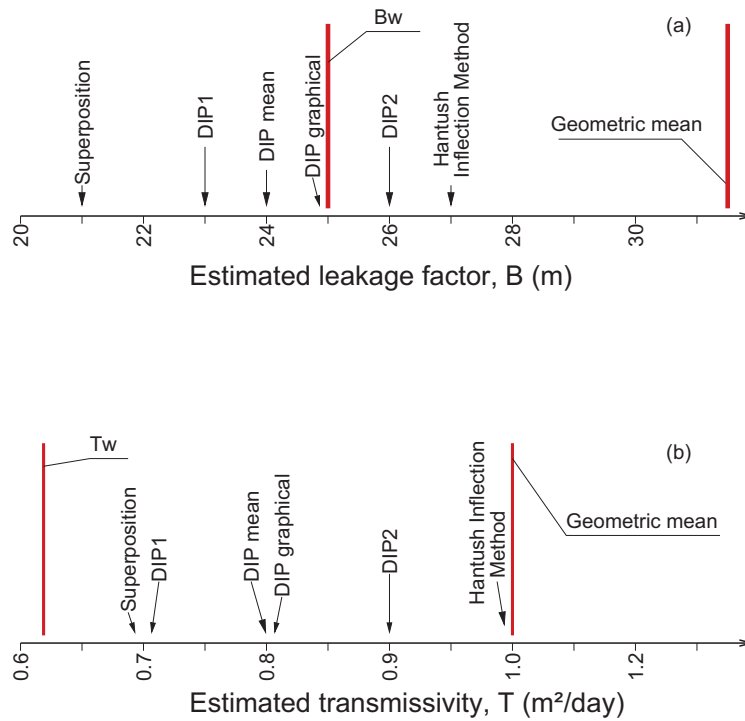


Figure 4.10: Estimates of the (a) leakage factor and (b) transmissivity using the different methodologies.  $B_w$  and  $T_w$  are the leakage factor and the transmissivity at the well, respectively.

#### 4.8 The Double Inflection Point Method as Indicator of Low/High Permeability at the Well

The example presented in the previous sections shows that in a heterogeneous system different interpretation methods provide different parameter estimates. Thus, using all methods may provide insight of the actual spatial variability of flow parameters. To illustrate this finding we consider two idealized heterogeneous leaky aquifer systems, one in which the transmissivity (and therefore the leakage factor) of the pumped aquifer has an increasing trend with distance from the well and the second in which the transmissivity trend is decreasing. The purpose of selecting such an idealized system, as opposed to a more realistic system with a complex spatial distribution, is that

the estimated parameters can be readily compared to the actual values used in the simulations. The transmissivity field, 1000 m by 1000 m, was generated using simple kriging with known mean and conditioned to the transmissivity value at the well. The mean transmissivity value was set to 1 *m/day* and the ratio between the transmissivity at the well,  $T_w$ , and the geometric mean of the transmissivity value is 2 in the first set of simulations and 0.5 in the second. The semivariogram is Gaussian with a range of 30 *m*. The storage coefficient is assumed to be uniform with a value of  $10^{-4}$ . The aquitard conductance is also assumed to be uniform. For each transmissivity field, two different simulations were carried out using different values of aquitard conductance ( $C=0.0001 \text{ day}^{-1}$  and  $C=0.001 \text{ day}^{-1}$ ).

The transient drawdown due to pumping at the center of the domain was simulated numerically. The simulated time-drawdown data at various points along a radial line from the well (since this example has radial symmetry) were used to estimate the parameters using the Hantush inflection point method and the DIP method using both  $t_{s1}$  and  $t_{s2}$ .

Figure 11 and 12 display the estimated leakage factor, normalized on the basis of the regional value (geometric mean) of  $T$ , as a function of the well distance.

At distances greater than 1-2 times the characteristic length of the transmissivity field (i.e. the range used in the definition of the transmissivity semivariogram which in this example is equal 30 *m*), the leakage factor estimated with the various methods approaches the regional value. Hence, in order to infer some information about the trend in transmissivity at the well, the observation points should be located at smaller distances from the well.

Figures 4.11 and 4.12 show that the leakage factor values estimated with the Hantush method are generally close to the actual values at the observation point. However, the Hantush inflection point method tends to overestimate the local value of the leakage factor when there is a decreasing trend of  $T$  with distance from the well, and underestimate the local value for an increasing  $T$  trend. The estimated values can be viewed as some average reflecting all transmissivity values from the

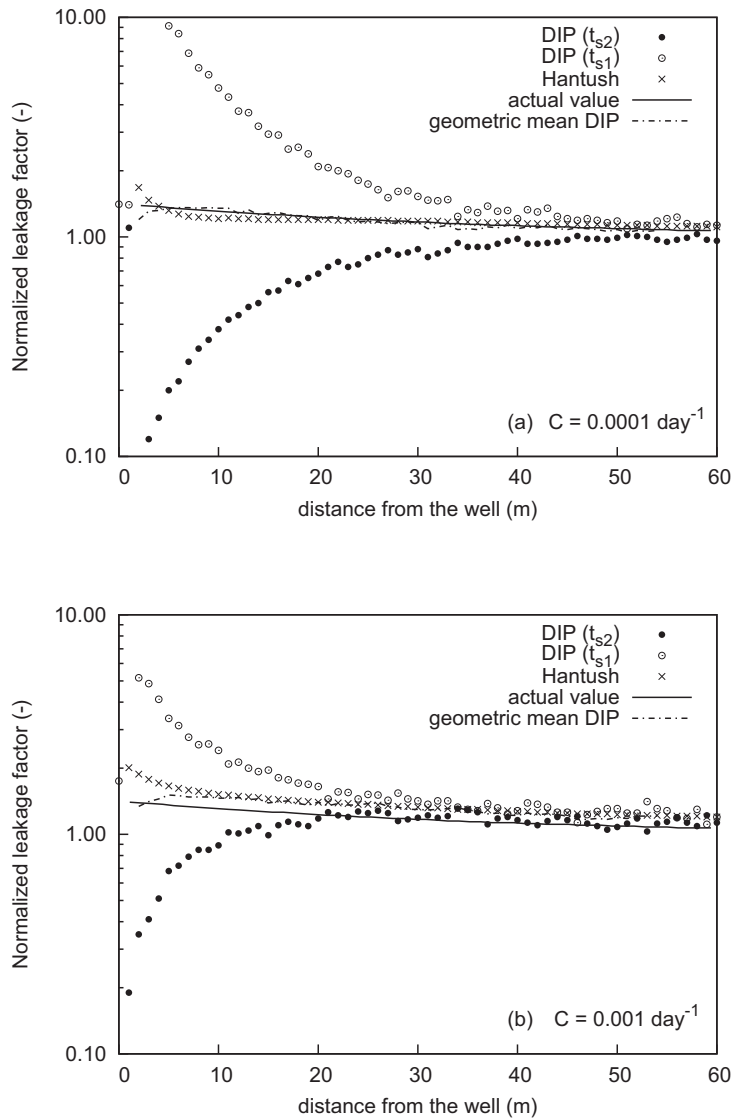


Figure 4.11: Leakage factor (normalized on the regional geometric mean of transmissivity) as a function of the well distance estimated using the DIP ( $t_{s1}$  and  $t_{s2}$ ) and Hantush inflection point methods. The ratio between the transmissivity at the well and the mean transmissivity value is 2.

well to the observation point and, hence, the decreasing/increasing trend extends for relatively large distances.

For small distances from the well, the DIP method (with both  $t_{s1}$  and  $t_{s2}$ ) is very sensitive to

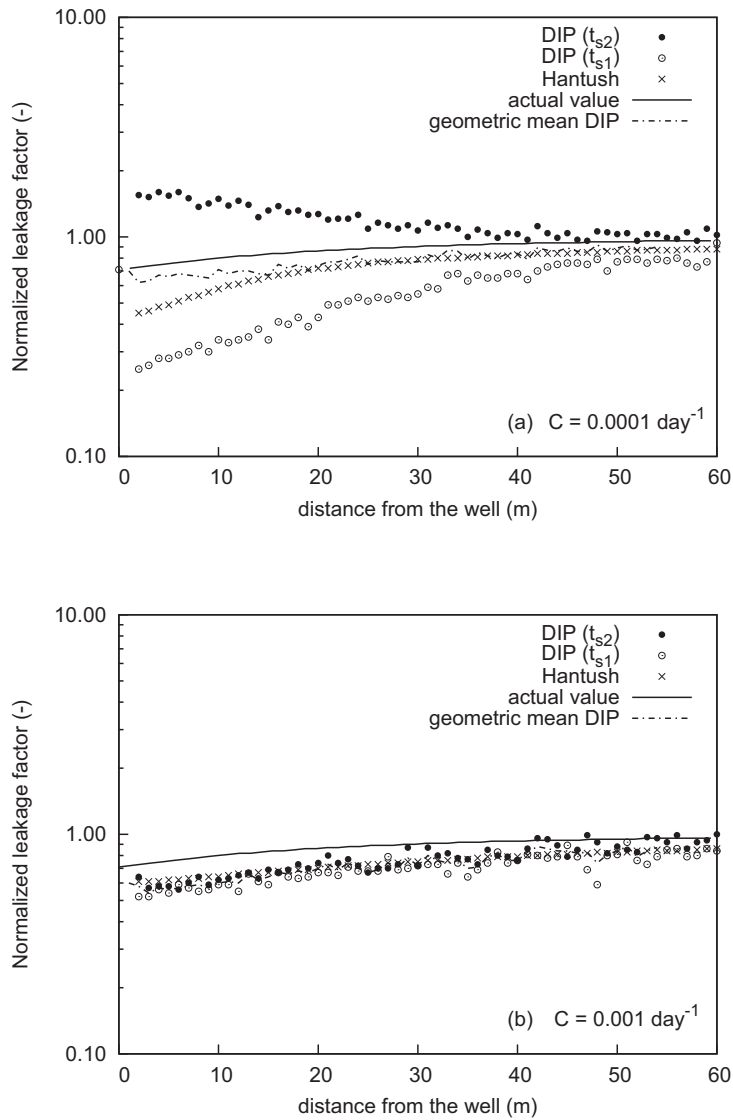


Figure 4.12: Leakage factor (normalized on the regional geometric mean of transmissivity) as a function of the well distance estimated using the DIP ( $t_{s1}$  and  $t_{s2}$ ) and Hantush inflection point methods. The ratio between the transmissivity at the well and the mean transmissivity value is 0.5.

trends in the transmissivity at the pumping well. When the well is located in a high-permeability zone, the DIP estimate based on  $t_{s1}$  is clearly overestimating the actual value of  $B$ , while the DIP estimate based on  $t_{s2}$  is underestimating the actual value. The opposite trend is observed when



the well is located in a low-permeability zone. Two important observations are noted: first, the geometric mean of the two estimations agrees quite well with the local leakage factor value, and second, some additional information, regarding the heterogeneous distribution of the values, is obtained precisely from the fact that the two estimates are different. The results described above suggest that the local transmissivity at the well is positively correlated with the DIP estimate based on  $t_{s1}$  and negatively correlated with the DIP estimate based on  $t_{s2}$ .

In leaky aquifers, the radius of the aquifer perturbed by the pumping test is controlled by the leakage factor. The ability of a pumping test to reveal information about the regional values of the aquifer depends on the value of the leakage factor relative to the characteristic length of the transmissivity field. With increase in the aquitard conductance, the leakage factor decreases, and the drawdown becomes influenced by the local flow parameters in the vicinity of the well. In Figure 4.11(a) for example, the leakage factor at the well is  $(2/0.0001)^{1/2} = 141$  m. The ratio of the leakage factor at the well to the transmissivity range (30 m) is close to 5, and the estimated leakage factor at large distances from the well is close to the regional value. In Figure 4.12(b), the leakage factor at the well is  $(0.5/0.001)^{1/2} = 22$  m. The ratio of the leakage factor at the well to the transmissivity range is about 0.75. Consequently, estimates from all methods are strongly influenced by the local flow parameters and identifying trends in the data may not be possible.

It should be pointed out that the estimates of the diffusivity ( $T/S$ ) in these examples were found to show similar trends to the leakage factor. The results are not presented here for brevity.

In conclusion the combined use of the DIP method and Hantush inflection point method allows for a semi-quantitative evaluation of the contrast between the local and regional transmissivity. This contrast may be related to the natural geological properties of the medium which means whether the well is located in a zone of high/low permeability.

The main novelty introduced by the DIP method is that a simple procedure using data from a single pumping test can be used to identify the contrast between the local and regional aquifer

transmissivity. The drawback is the need for carefully monitored continuous data, since noise in head data and natural trends such as barometric pressure and tidal fluctuations can strongly influence the estimation of higher order derivatives in the drawdown signal. The need for unaffected piezometers must be taken into account when designing the network of observation points.

## 4.9 Summary

A new methodology for the interpretation of a pumping test in a leaky aquifer, referred to as the Double Inflection Point (DIP) method, is developed. The method is based on the leaky aquifer system defined by *Hantush and Jacob* [44]. The main advantage of the method is that it does not involve any curve fitting, requiring instead the estimation of the position of three points on the time-drawdown curve, namely the times where the first and second derivatives of the drawdown as a function of log time are maximum/minimum. The main limitation of the method is that it requires the evaluation of the first and second derivatives of the drawdown which are sensitive to errors in the observed head measurements. Furthermore, frequent measurements of the data would also be needed to accurately identify the singular points of the time-drawdown data.

When applied to homogeneous media, the DIP method yields the exact parameters of the aquifer and aquitard ( $T$ ,  $S$  and  $B$ ); as is the case with other methods such as the Hantush Inflection point method and Walton type-curve method. The primary benefit of the DIP method is when applied to heterogeneous media where each method provides different and valuable indirect information about the heterogeneous distribution of the local transmissivity values.

A synthetic pumping test was performed in a heterogeneous medium and interpretation of the results shows that each method is influenced differently by the transmissivity of the aquifer volume surrounding the well. The methods which use mainly the first part of the drawdown curve provide an estimated value which is close to the actual one at the well, while those which analyze the late transient part of the curve give an estimate that averages the local and the equivalent value of the

entire aquifer.

In short, we show that near the well and for leakage factor greater than the characteristic length of the transmissivity field, the coupled use of the DIP method and the Hantush inflection point method can identify a potential high/low permeability zone near the pumping well if present. Because different interpretation methods yield similar results at large distances from the well, the information provided by the piezometers located near the well is most useful in the characterization of these contrasts in the permeability.

#### 4.10 Appendix - Symmetry of the Second Derivative of the Draw-down Curve

Substituting  $\tau_j = 1/4\lambda_i$  ( $j = 1, 2$  and  $i = 3 - j$ ) in Equation 4.13 and rearranging terms, we obtain:

$$B = \frac{\left(\lambda_i^2 - \frac{1}{4}\right)^2 r}{\lambda_i \left(\lambda_i^2 + \frac{1}{4}\right)} \quad (4.22)$$

Comparing Equation 4.22 with Equation 4.13, we can state that  $\tau_j$  and  $\lambda_i = 1/4\tau_j$  are the two real roots of Equation 4.11.

From its definition,  $\lambda_i$  is related to  $\tau_j$  by the following relationship:

$$\lambda_i \tau_j = 1/4 \quad (4.23)$$

If we express these two terms using the definition of  $\tau_j$ , we obtain an explicit relation that relates the three singular points  $t_{sj}$ ,  $t_{si}$ , and  $t_{inf}$ :

$$t_{sj}t_{si} = t_{inf}^2 \quad (4.24)$$

that is:

$$\log t_{sj} - \log t_{inf} = \log t_{inf} - \log t_{si} \quad (4.25)$$

Equation 4.25 indicates that, on a logarithmic plot, the positions of the two inflection points of the first derivative of the drawdown curve (Equation 4.8) are symmetric with respect to the position of  $t_{inf}$ .

#### 4.11 Appendix - Sensitivity Analysis of the DIP Method

In this Appendix, the sensitivity of the DIP method in the estimation of the location of the inflection points is assessed. Denoting  $\nu = \tau_j$  for brevity, the derivative of  $B$  appearing in equation (4.13) with respect to  $\nu$  is

$$\frac{\partial B}{\partial \nu} = \frac{(\nu^2 - 1/4)^2}{(\nu^2 + 1/4)} \left[ -\frac{1}{\nu^2} - \frac{2}{\nu^2 + 1/4} + \frac{4}{\nu^2 - 1/4} \right] r \quad (4.26)$$

Combining equation (4.13) and (4.26) yields

$$\frac{\partial B}{B} = \frac{\partial \nu}{\nu} \left[ \frac{4\nu^2}{\nu^2 - 1/4} - \frac{2\nu^2}{\nu^2 + 1/4} - 1 \right] \quad (4.27)$$

Since  $r/B$  is a function of  $\nu$  only, equation (4.27) permits the evaluation of the error in the estimation of the leakage factor as a function of  $r/B$  and the error in the evaluation of  $\nu$ .

The error curve is displayed in Figure 4.7 for a relative error of 10% and 25% in the estimation of

*v.* The two errors are almost equal up to a value of  $r/B \cong 0.5$ . For  $r/B$  larger than 2, the error in  $B$  starts to increase rapidly. Therefore, the error of the DIPM would be moderate for most realistic cases of  $r/B$ , since generally  $B$  is on the order of tens to hundreds of meters, while the observation points are usually located close to the well (tens of meters at most).